ELECTRONIC SUPPLEMENTARY INFORMATION

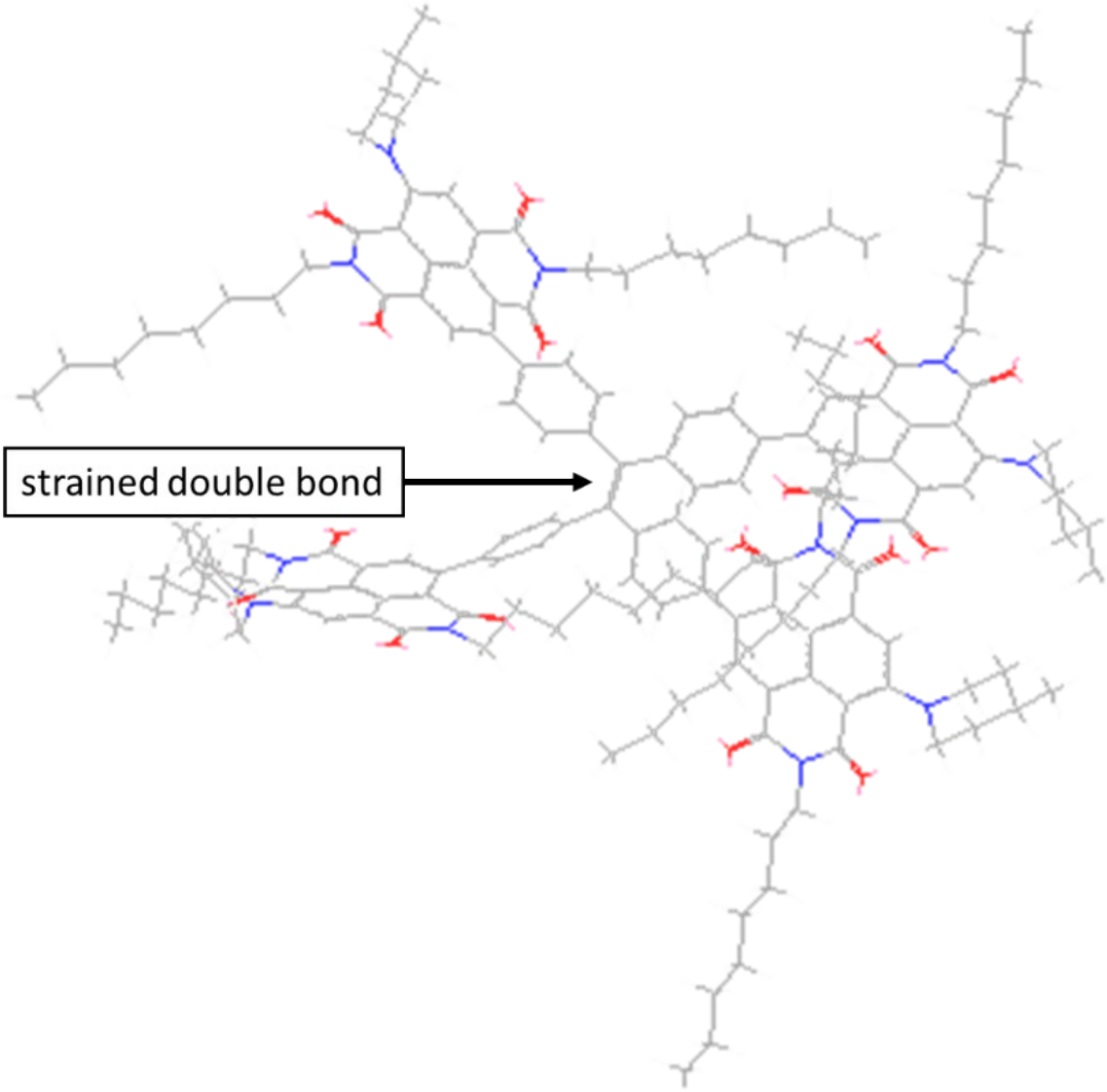

Fig. S1 Three-dimensional, wired structure of **W8** showing strained double bond.

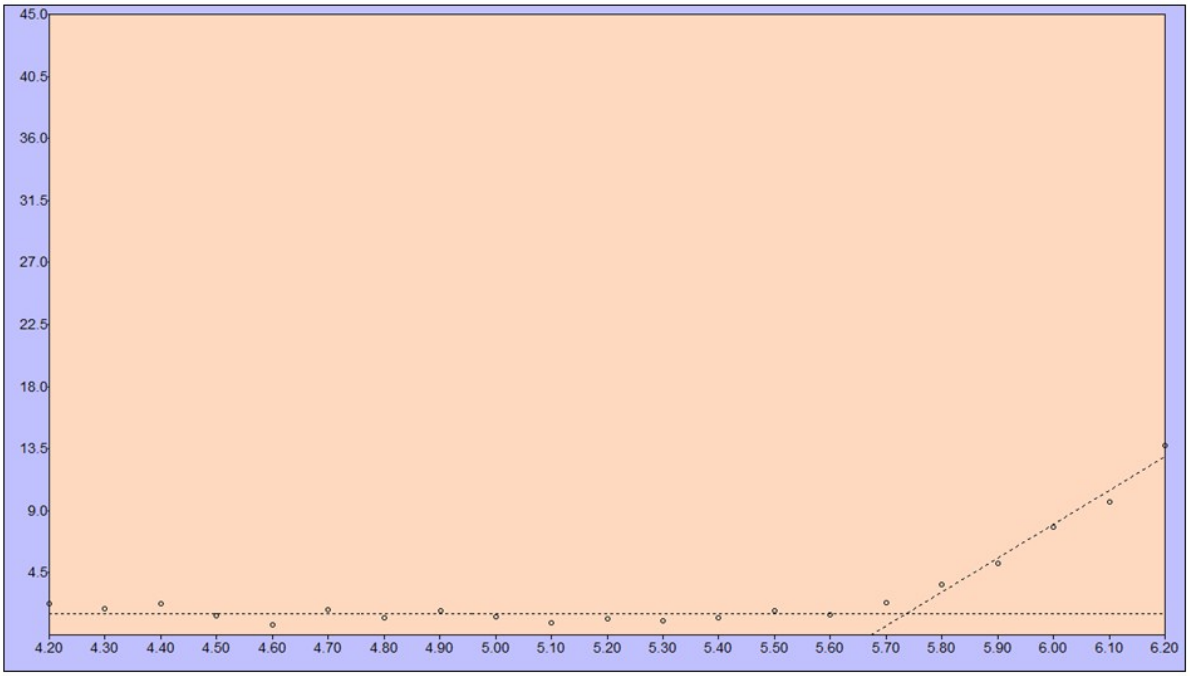

Fig. S2 PESA spectrum of thin film of **W8**. The dashed-lines show the fits to extract ionisation potential (-5.73 eV) which corresponds to the HOMO energy level.

Details of DFT Calculations

The Gaussian 09 *ab initio*/DFT quantum chemical simulation package was employed to get results described in the present work.[S1] The geometry optimization of **W8** has been carried out at the B3LYP/6-31G(d) level of theory. To ensure the structures to be real, frequency calculations were carried out. Furthermore, the geometries of **W8** obtained at the B3LYP/6-31G(d) level were subjected to the time-dependent density functional theory (TD-DFT) studies using the M062X/6-31G(d).[S2,S3] TD-DFT results obtained for **W8** are reported in Table S1. From the TD-DFT results it is seen that **W8** shows two major absorption peaks at 445 nm and 321 nm. The frontier molecular orbitals (FMOs) were generated using Avogadro.[S4,S5]

Table S1 Calculated TD-DFT excitation properties of **W8**.

Material	**Excitation Energy (eV)**	**Excitation Wavelength (nm)**	**Oscillator Strength (f)**	**Excitations**	**% contribution for transition**
W8	2.7858	445.05	0.5010	492 → 497	H-4 → LUMO (13%)
				492 → 498	H-4 → L+1 (3%)
				493 → 497	H-3 → LUMO (21%)
				494 → 498	H-2 → L+1 (4%)
				495 → 498	H-1 → L+1 (2%)
				496 → 497	HOMO → LUMO (30%)
				496 → 498	HOMO → L+1(14%)

	3.8528	321.80	0.4864	482 → 497	H-14 → LUMO (3%)
				482 → 498	H-14 → L+1 (2%)
				483 → 497	H-13 → LUMO (22%)
				484 → 498	H-12 → L+1 (16%)
				485 → 498	H-11 → L+1 (27%)
				486 → 499	H-10 → L+2 (4%)
				487 → 500	H-9 → L+3 (7%)

Frontier molecular orbitals of **W8** with energy levels in eV

W8		**eV**	
L+4	501	-0.67648	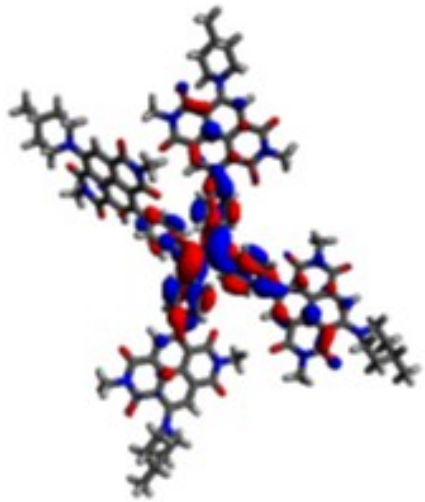
L+3	500	-2.20849	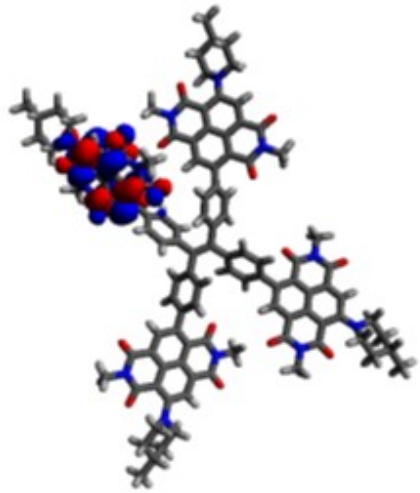

L+2	499	-2.23026	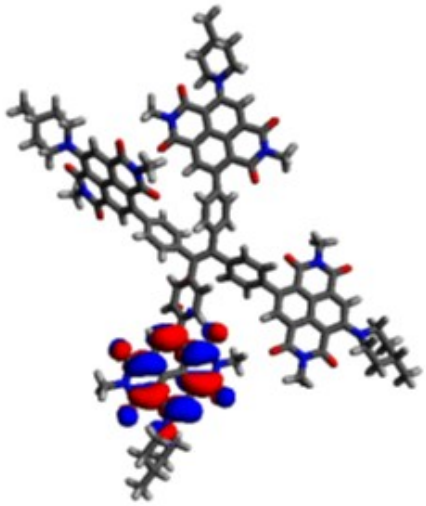
L+1	498	-2.32605	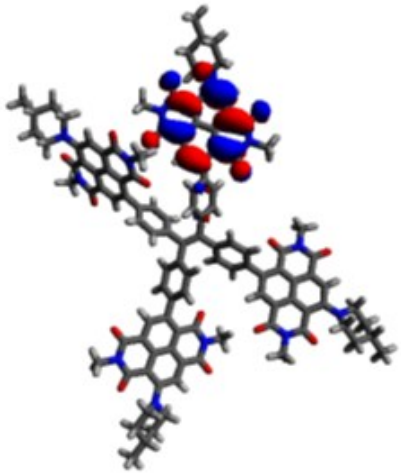
L	497	-2.35163	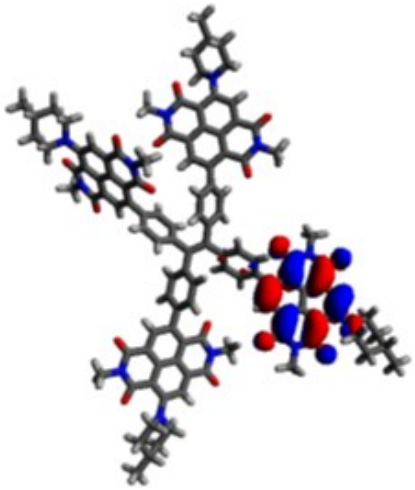

H	496	-6.37949	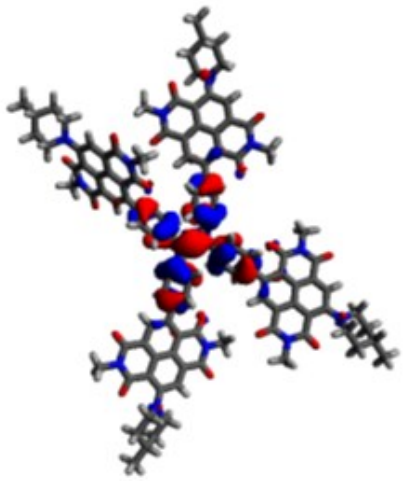
H-1	495	-7.02141	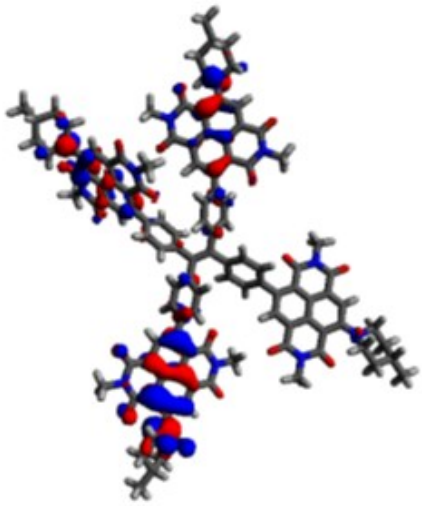
H-2	494	-7.04345	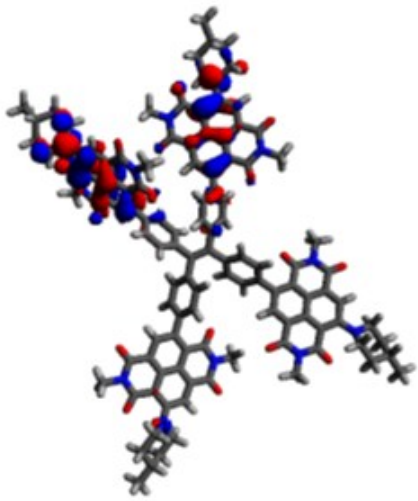

H-3	493	-7.06059	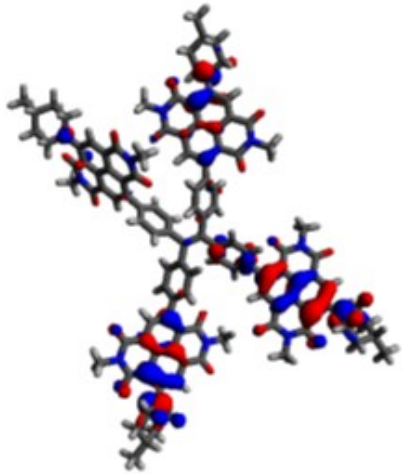
H-4	492	-7.16998	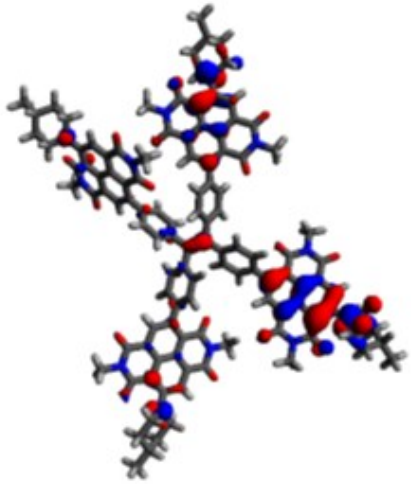
H-5	487	-8.05463	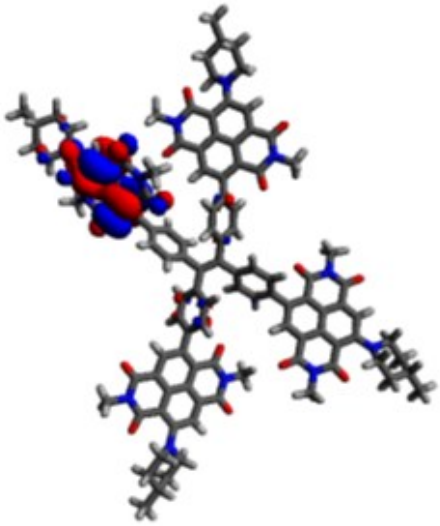

H-10	486	-8.07559	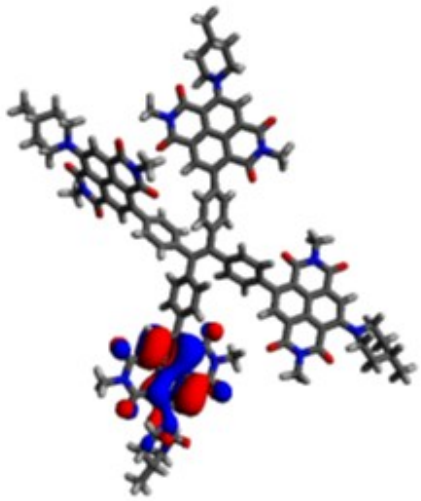
H-11	485	-8.14117	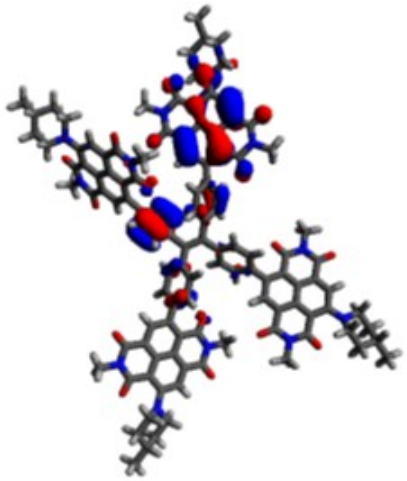
H-12	484	-8.15749	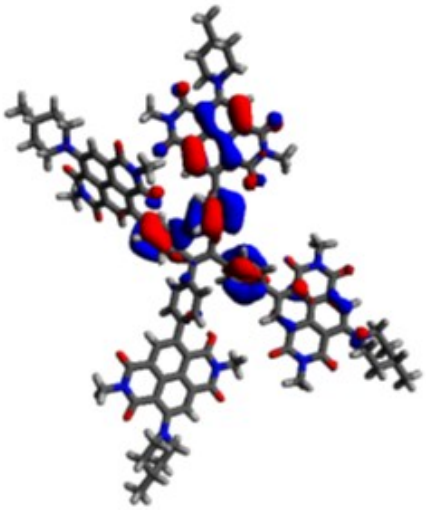

H-13	483	-8.17981	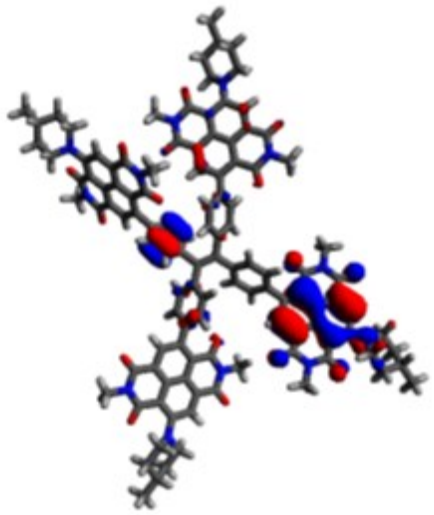
H-14	482	-8.20675	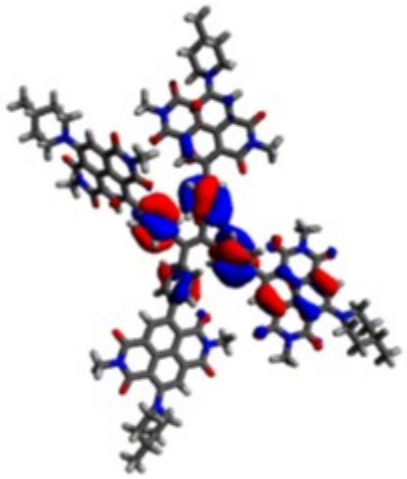

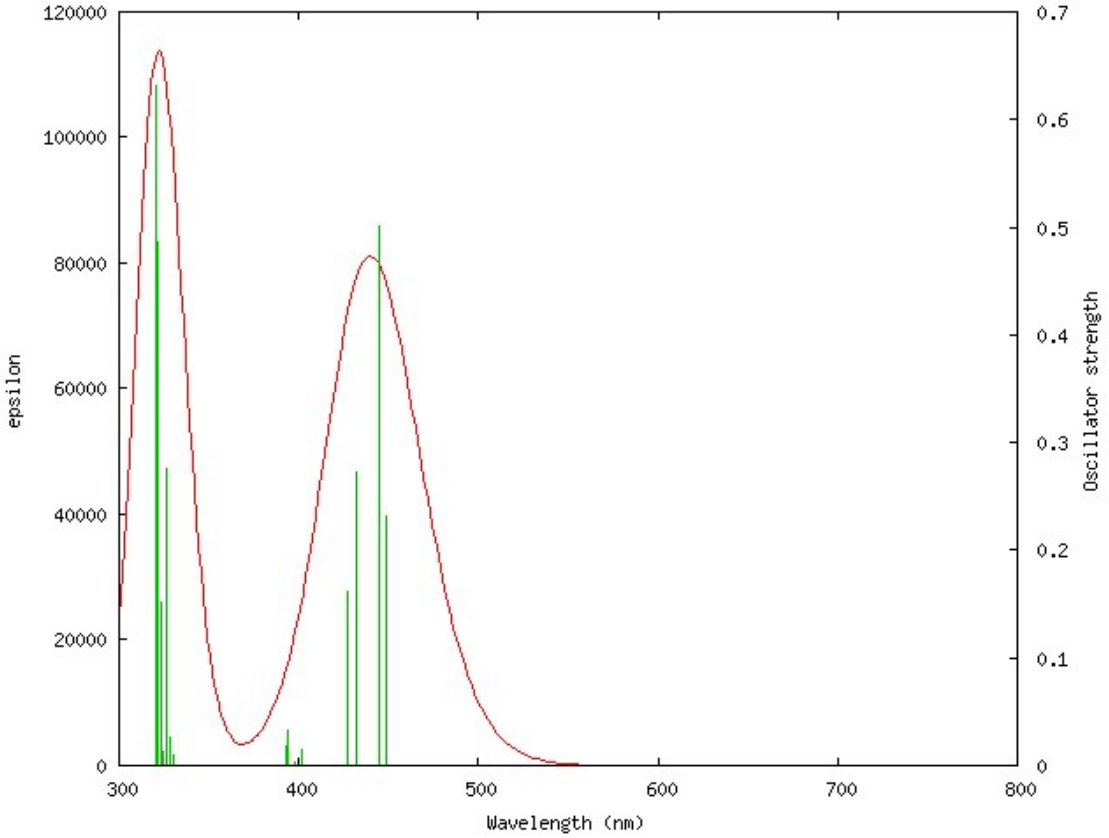

Fig. S3 Computed absorption spectrum of **W8** showing transition peaks at 445 nm and 321 nm.

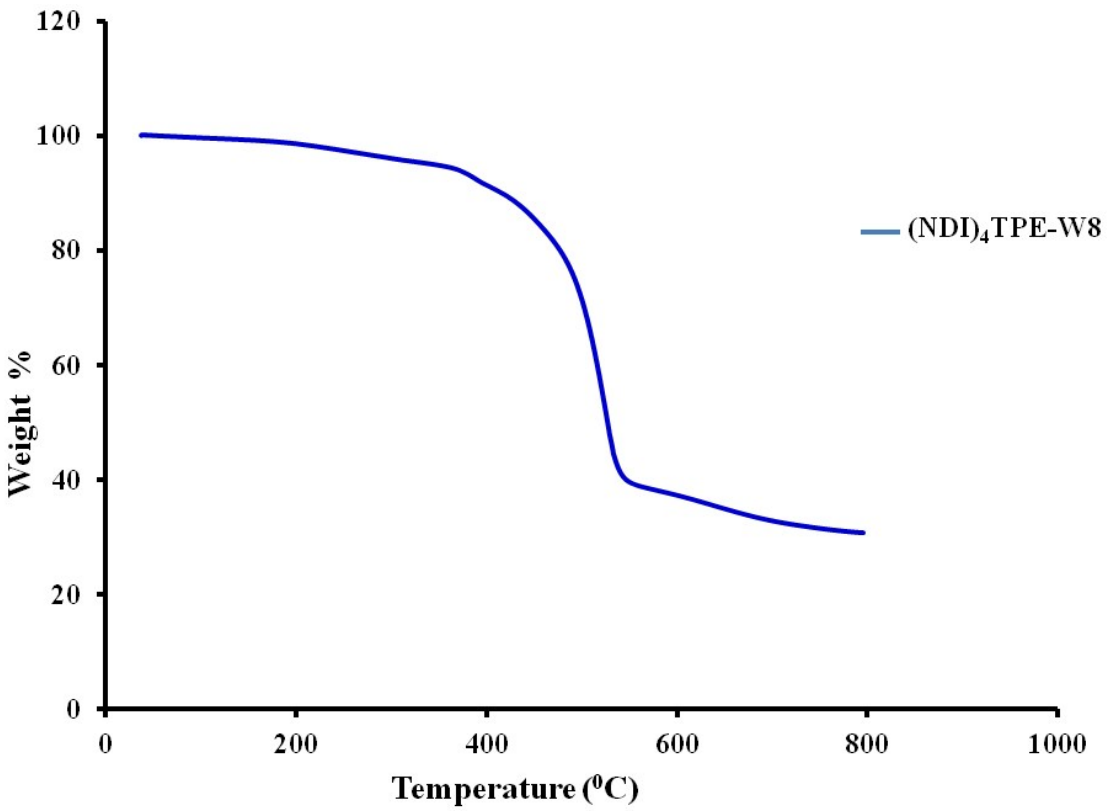

Fig. S4 Thermogravimetric analysis curve showing thermal stability of **W8**.

Table S2. Photovoltaic cell parameters for **W8** blends

Acceptor	**Donor**	**Testing conditions (D: A)**[a]	V_{oc} **(V)**	J_{sc} **(mA/cm^2)**	***FF***	**Best PCE (%)**	**Average PCE (%) (± std dev)**
W8	PTB7	1: 1.2 (no annealing)	0.94	10.21	0.60	5.72	5.63 (± 0.06)
W8	PTB7	1: 1.2 (annealed)	1.04	13.41	0.62	8.58	8.51 (± 0.05)
W8	P3HT	1: 1.2 (annealed)	0.95	9.24	0.60	5.26	5.18 (± 0.06)
$PC_{61}BM$	P3HT	1: 1.2[b]	0.57	8.28	0.64	3.03	2.99 (± 0.04)

[a] BHJ devices with specified weight ratio. Device structure was ITO/PEDOT: PSS (38 nm)/active layer/Ca (20 nm)/Al (100 nm) with an active layer thickness of ~75 nm; [b] A standard P3HT: $PC_{61}BM$ device afforded 3.03% efficiency when tested under alike annealing conditions.

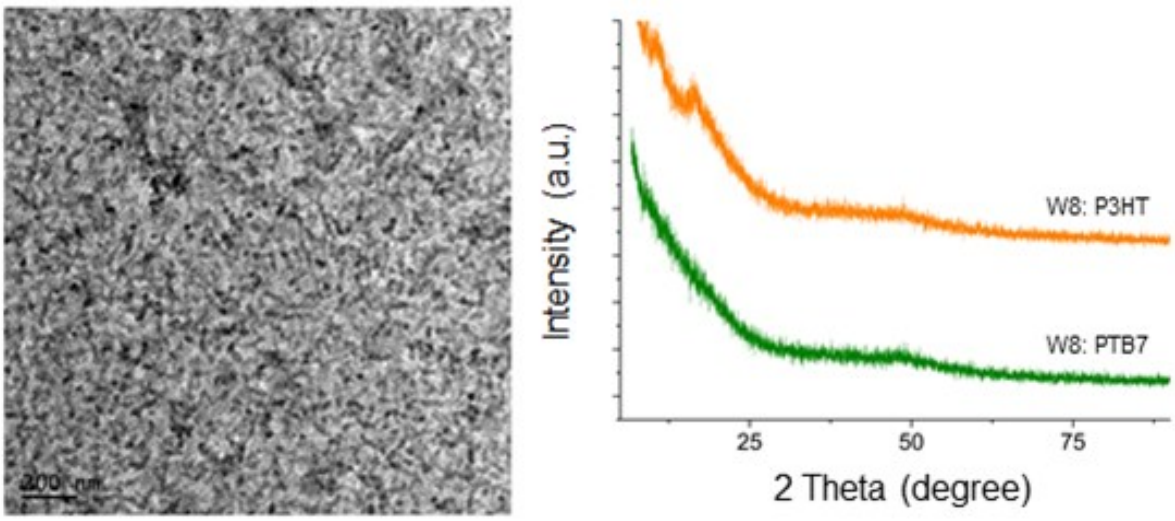

Fig. S5 TEM (left) and XRD (right) images for the active blend surfaces of **W8**. The TEM image shows an excellent intermixing of donor and acceptor domains (PTB7: **W8** 1: 1.2; scale bar = 200 nm), whereas XRD spectra indicate the blend surfaces to be amorphous.

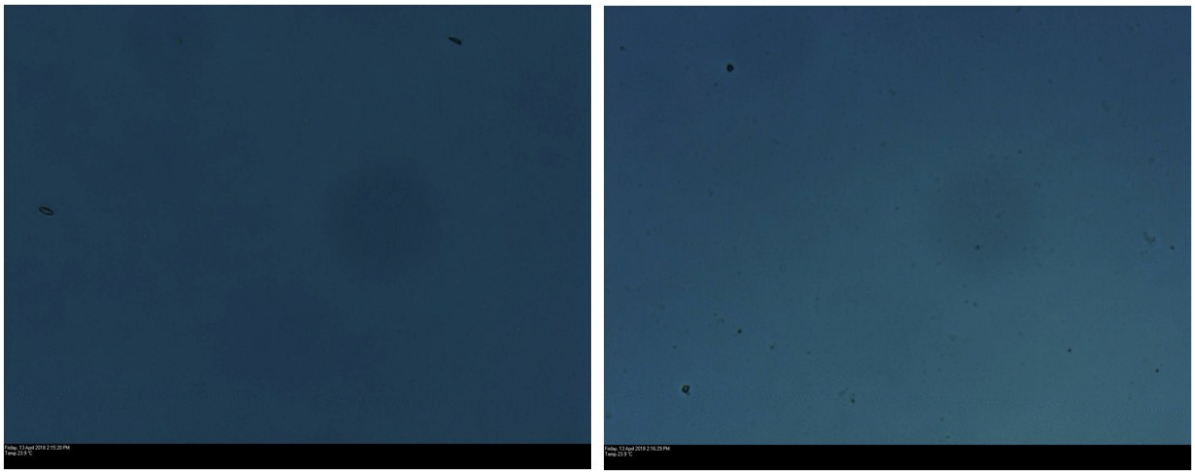

Fig. S6 Optical microscopic images for the blend surfaces of **W8** (P3HT left and PTB7 right) showing fairly flat surfaces corroborating TEM and XRD analyses.

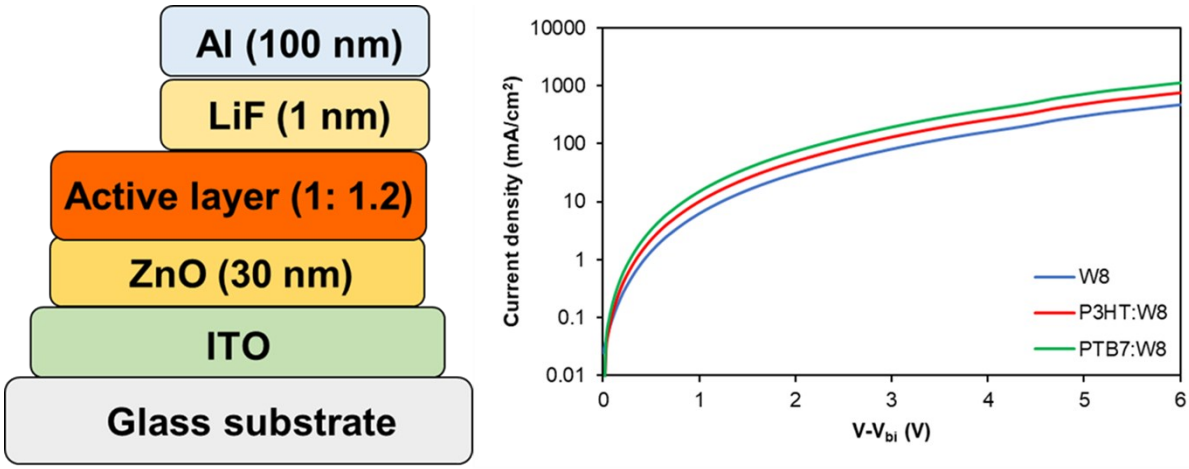

Active layer	Electron Mobility (cm^2/Vm)
W8	1.20×10^{-3}
PTB7: W8	4.61×10^{-3}
P3HT: W8	2.17×10^{-3}

Fig. S7 Current–voltage characteristics of electron only devices which were applied to Mott-Gurney equation to calculate electron mobilities of **W8** and its blends.

Experimental spectra

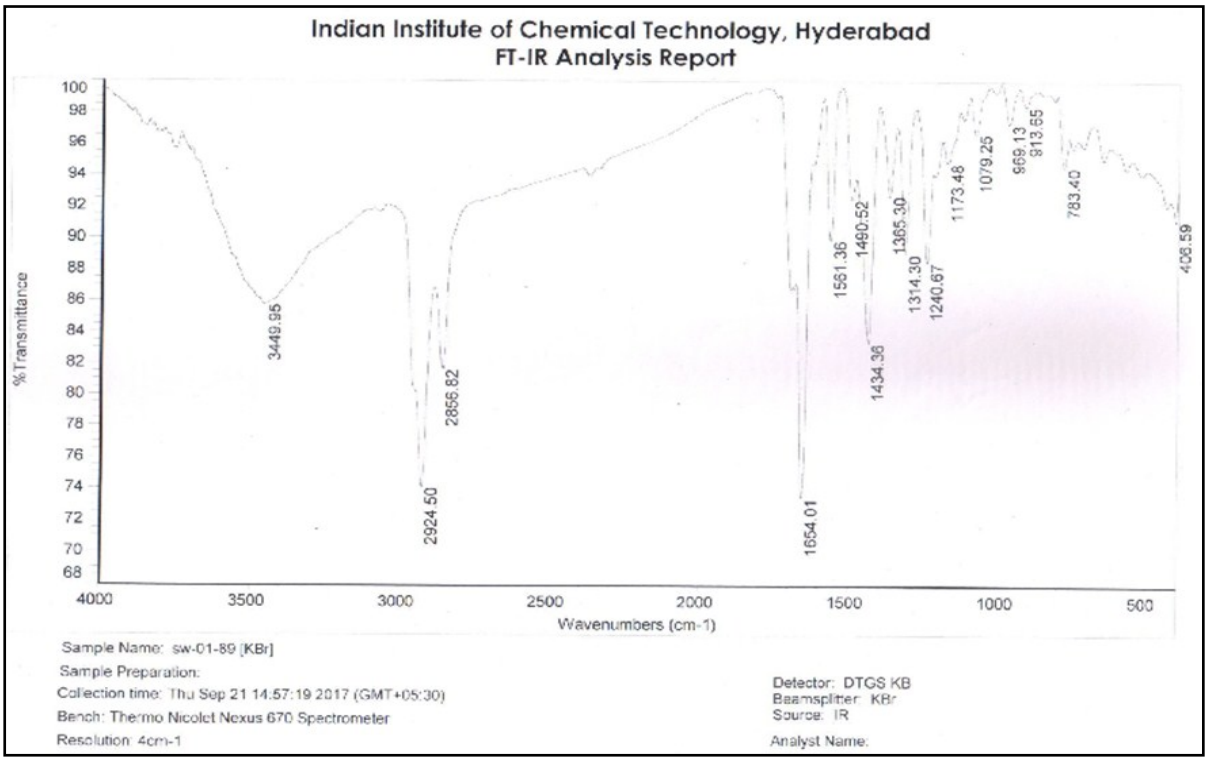

Fig. S8 FT-IR spectrum of compound **1.**

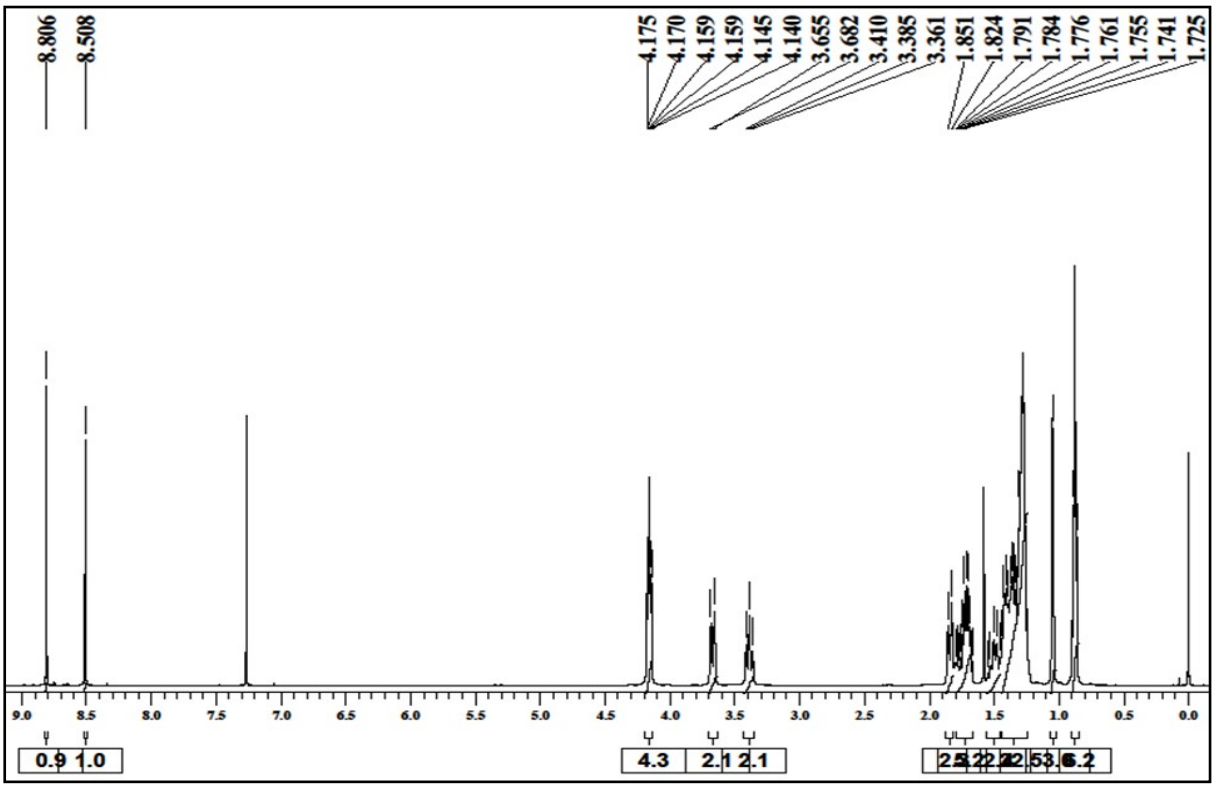

Fig. S9 ^{1}H NMR spectrum of compound **1.**

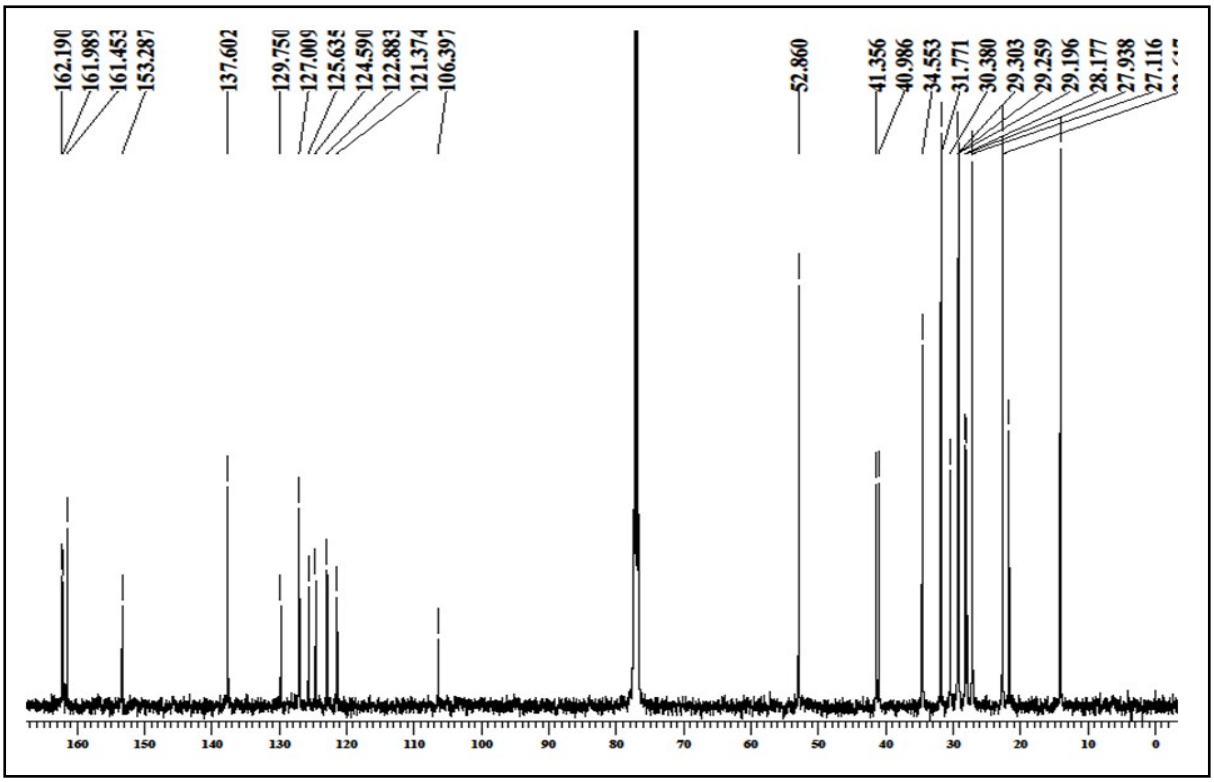

Fig. S10 ^{13}C NMR spectrum of compound **1.**

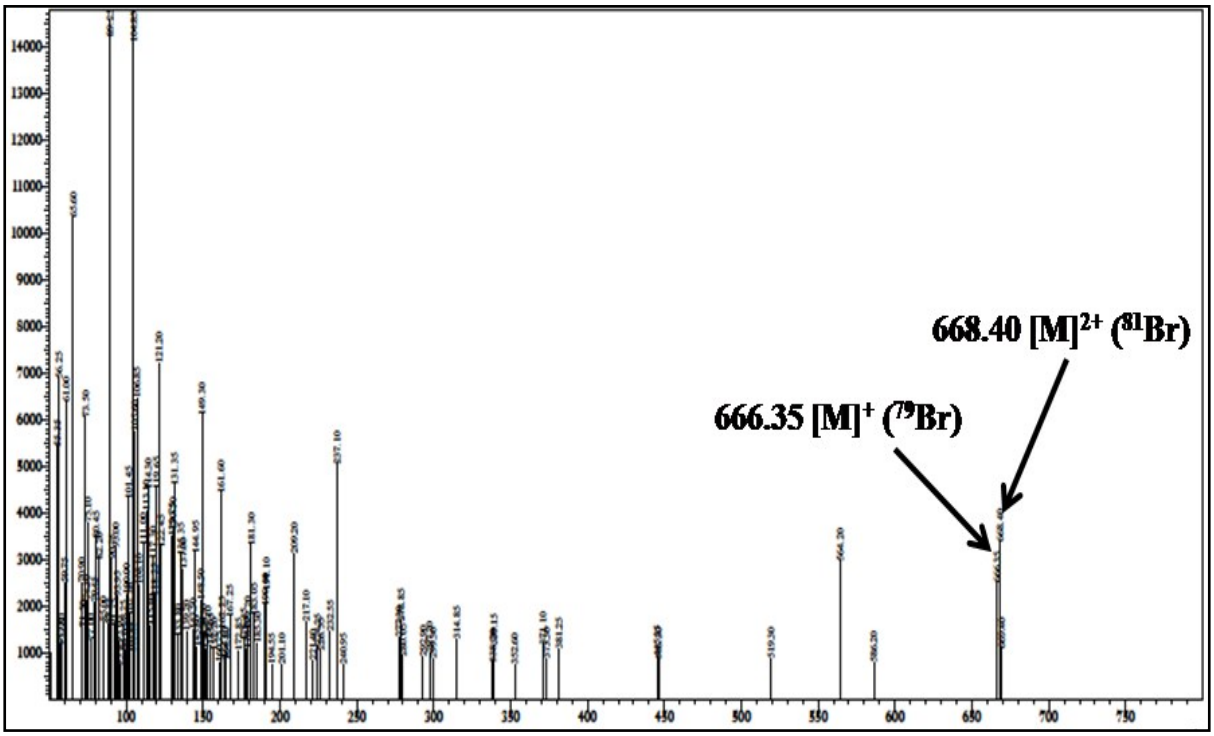

Fig. S11 ESI-MS spectrum of compound **1.**

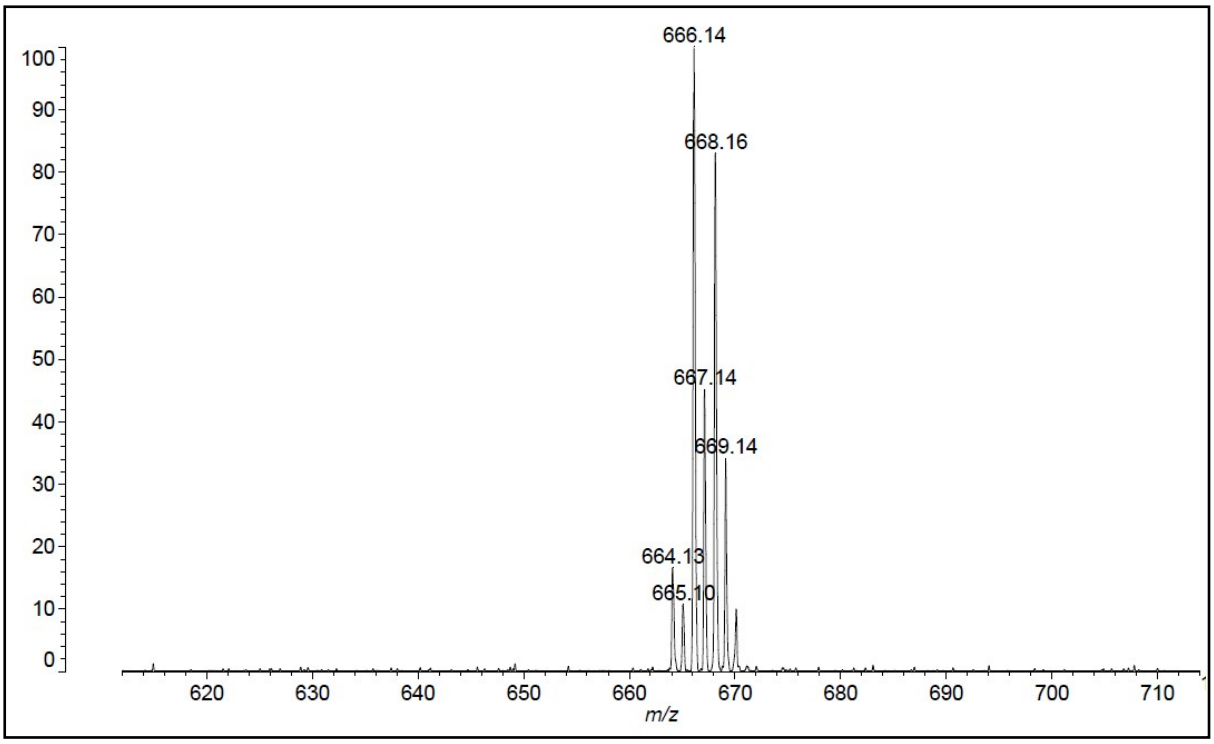

Fig. S12 MALDI-TOF spectrum of compound **1.**

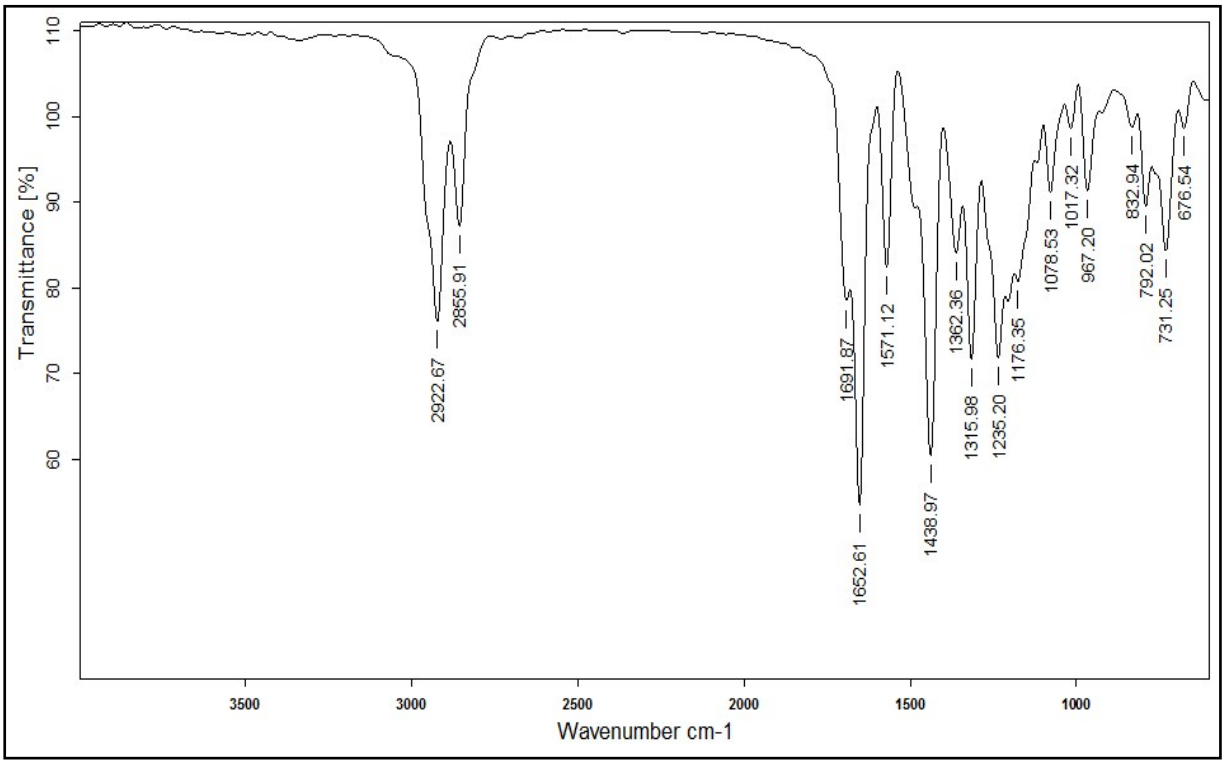

Fig. S13 FT-IR spectrum of **W8**.

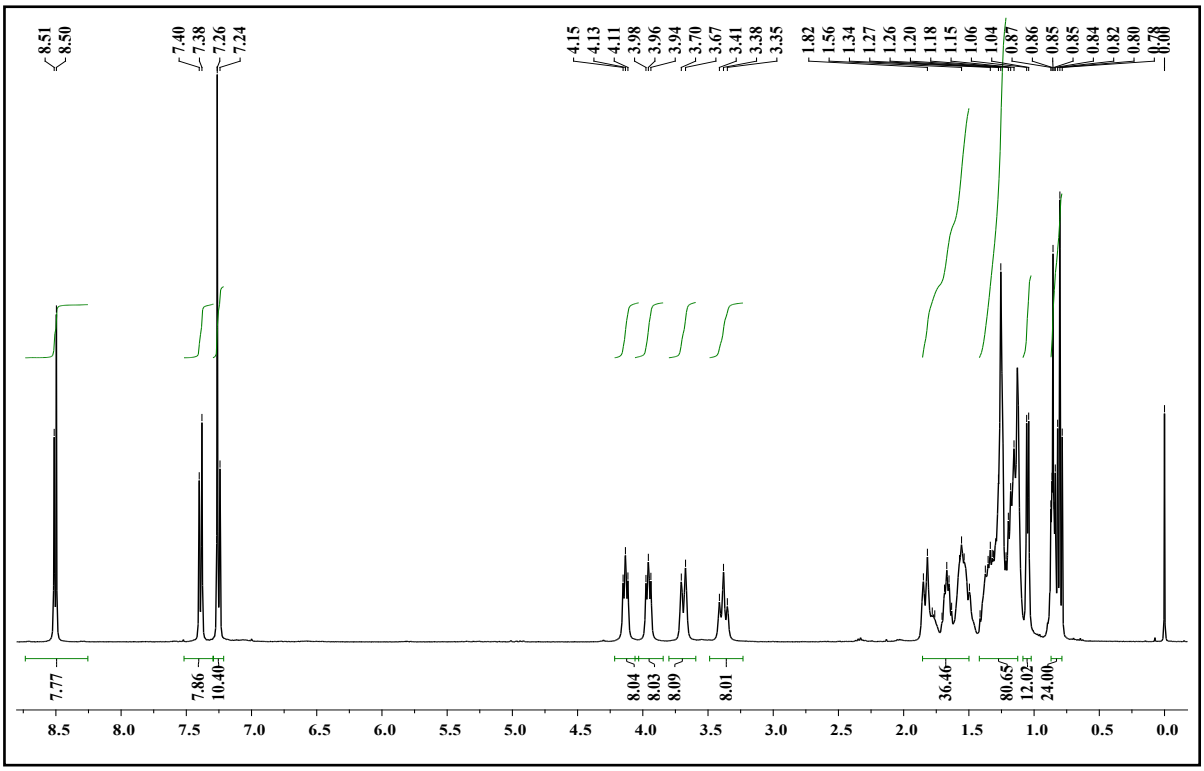

Fig. S14 ^{1}H NMR spectrum of **W8**.

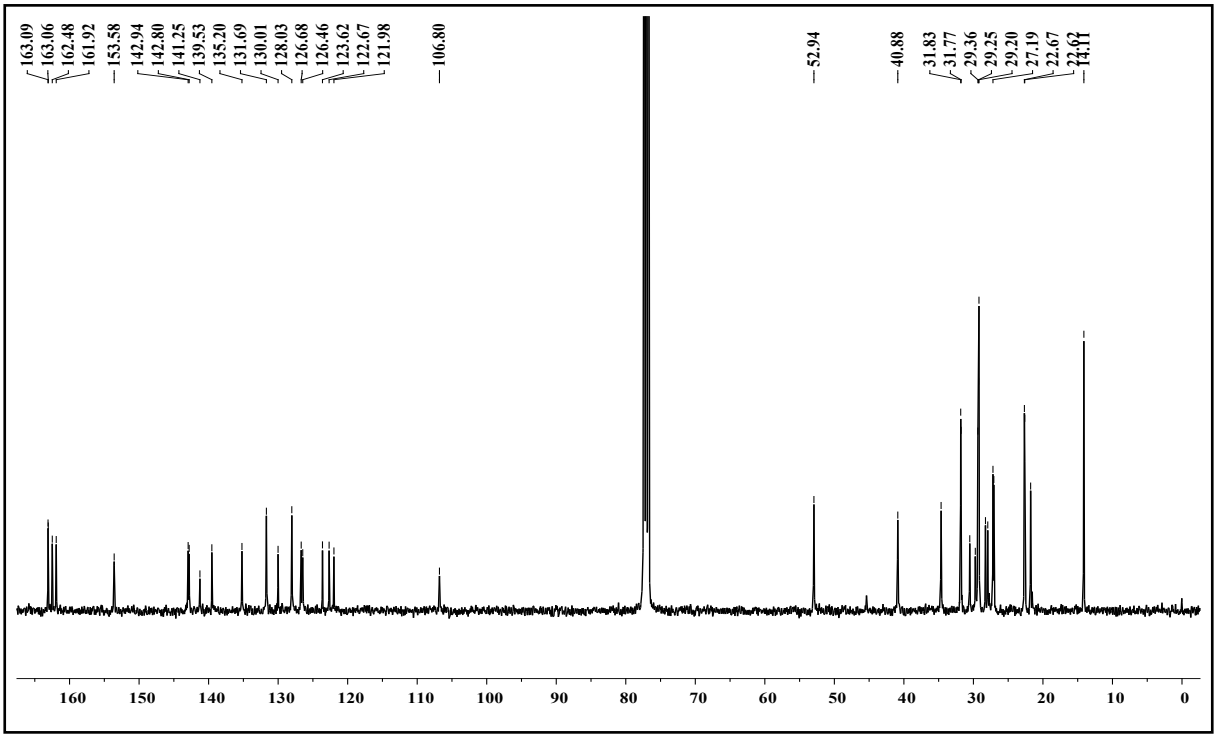

Fig. S15 ^{13}C NMR spectrum of **W8**.

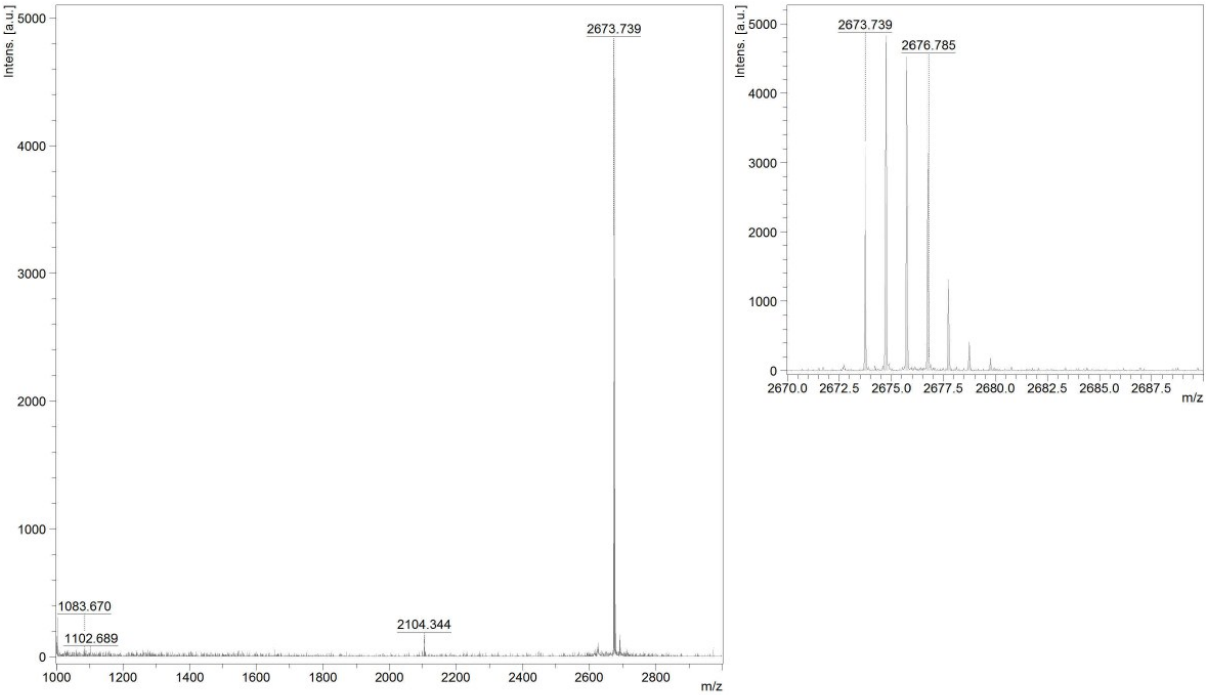

Fig. S16 MALDI-TOF spectrum of **W8**.

References:

S1 M. J. Frisch, *et al.*, *Gaussian 09*, *Revision C.01*, Gaussian Inc., Wallingford CT, 2009.
S2 Y. Zhao, *et al.*, *Chem. Phys. Lett.*, 2011, 502, 1.
S3 D. Srivani, *et al.*, *Dyes Pigm.*, 2017, 143, 1.
S4 Avogadro: an open-source molecular builder and visualization tool, Version 1.1.0. http://avogadro.openmolecules.net/
S5 M. D. Hanwell, *et al.*, *J. Cheminf.*, 2012, 4, 17.